DOI: 10.5604/01.3001.0013.7936

Volume 96 • Issue 2 • October 2019

Journal of Achievements in Materials and Manufacturing Engineering

International Scientific Journal published monthly by the World Academy of Materials and Manufacturing Engineering

Physical and chemical mechanisms of hydrophobicity of nanoparticle membranes (Mg+Al_2O_3)

Wahyudi [a], R. Subagyo [b,*], F. Gapsari [c]

[a] Department of Mechanical Engineering, Faculty of Engineering,Universitas Muhammadiyah Yogyakarta, Brawijaya street, Kasihan, Bantul, Yogyakarta, 55183, Indonesia

[b] Mechanical Engineering Department, Engineering Faculty, University Lambung Mangkurat, Jenderal Achmad Yani Street KM 35.5, Banjarbaru, South Kalimantan, 70714, Indonesia

[c] Mechanical Engineering Department, Engineering Faculty, University Brawijaya, Veteran street No. 16, Malang, East Java, 65145, Indonesia

* Corresponding e-mail address: rachmatsubagyo@ulm.ac.id

ABSTRACT

Purpose: Investigate the hydrophobic, superhydrophobic and hydrophilic properties of Alumina (Al_2O_3) and Magnesium (Mg) nanoparticles.

Design/methodology/approach: This research was conducted by SEM-EDX analysis of Magnesium and Alumina nanoparticles, observation of gas bubbles when droplets of water contact with membrane surfaces, measurement of surface roughness and detection of Hydrogen gas production using Gas Chromatography. There are eleven compositions (Al_2O_3:Mg) membranes used in this study, namely: (0:100; 10:90; 20:80; 30:70; 40:60; 50:50; 60:40; 70:30; 80:20; 90:10; and 100:0).

Findings: Successfully found an alloy membrane between Alumina (Al_2O_3) and Magnesium (Mg) nanoparticles in the composition of Mg:Al_2O_3 (0:100%) having Hydrophobic properties; Mg:Al_2O_3 (50:50%) has Superhydrophobic properties and Mg:Al_2O_3 (100:0%) has hydrophilic properties. Three conditions occur when H_2O droplets come in contact with the membrane layer, namely: hydrophobic conditions when the trapped gas pressure is smaller than the droplet pressure. Superhydrophobic conditions when the trapped gas pressure is equal to the droplet pressure. Hydrophilic conditions occur when the trapped gas pressure is greater than the droplet pressure.

Research limitations/implications: This research is limited to the hydrophobic nature of Nano Alumina (Al_2O_3) and Magnesium (Mg) membrane particles.

Practical implications: Superhydrophobic properties are very suitable to be applied to membranes that are useful for destiny.

Originality/value: The novelty of this study is to find the right mixture of nanoparticles of Alumina and Magnesium in a composition that is capable of creating hydrophobic, superhydrophobic and hydrophilic properties.

Keywords: Hydrophobic, Superhydrophobic, Hydrophilic, SEM-EDX, Gas bubbles, Nanoparticles, Membranes

Reference to this paper should be given in the following way:
Wahyudi, R. Subagyo, F. Gapsari, Physical and chemical mechanisms of hydrophobicity of nanoparticle membranes (Mg+Al_2O_3), Journal of Achievements in Materials and Manufacturing Engineering 96/2 (2019) 57-68.

1. Introduction

Wetting is the ability of liquids to maintain contact with solid surfaces, which results from intermolecular interactions when the two are combined. The contact angle formed when dripping liquid onto the surface of a solid/membrane is very closely related to the hydrophobicity of a material. The degree of hydrophobicity of a material is determined by the balance between adhesive strength and cohesive strength. Hydrophobicity occurs due to collaboration between three phases of material, namely: gas, liquid, and solid. The hydrophobicity process of material is now the centre of attention in nanotechnology and the study of nano-science is due to the growing development of nano-material research.

The main parameter of hydrophobicity of a material is the static contact angle, which is defined as the angle formed between a liquid and a solid. The contact angle depends on several factors, such as surface energy, surface roughness, and cleanliness [1-6]. If the liquid wets the surface is called a hydrophilic surface, the static contact angle value is $0 \leq \theta \leq 90°$, whereas if the liquid does not wet the surface is called a hydrophobic surface, the value of the contact angle is $90° < \theta \leq 180°$.

The hydrophobicity of material is also indicated by the value of the contact angle, hysteresis contact angle, and shear angle. The contact angle (θ) is the angle formed by a tangent to the liquid in the contact line and a line through the base of the liquid drops. According to [7-10] the profile of water drops and contact angles (θ) that occur in materials classified into 4 are: superhydrophilic ($\theta \approx 0$), hydrophilic ($\theta < 90°$), hydrophobic ($90° < \theta < 120°$), ultrahydrophobic ($120° < \theta < 150°$) and superhydrophobic ($\theta > 150°$).

The hydrophobic nature of a material is its ability to reject water (water repellent) [11], self-cleaning [12] and its ability to reduce barriers [13,14]. Various kinds of superhydrophobic surfaces have been produced at the laboratory scale and some have even been produced commercially [15-17]. Such as medical equipment that is hemocompatibility [18], waterproof textile [19], membrane distillation [7], Self lubrication material [20], and as a corrosion protection material [21].

Based on previous research there are several models on the hydrophobic nature of a material, namely:

a) Young model (Fig. 1)

The application of this equation is for flat, smooth and homogeneous surfaces [22,23]:

$$Cos\ \theta = \frac{(\gamma_{SV} - \gamma_{SL})}{\gamma_{LV}} \tag{1}$$

where:
γ_{LV}: liquid-vapour interface tension,
γ_{SL}: liquid-solid interface tension,
γ_{SV}: vapour-solid interface stress.

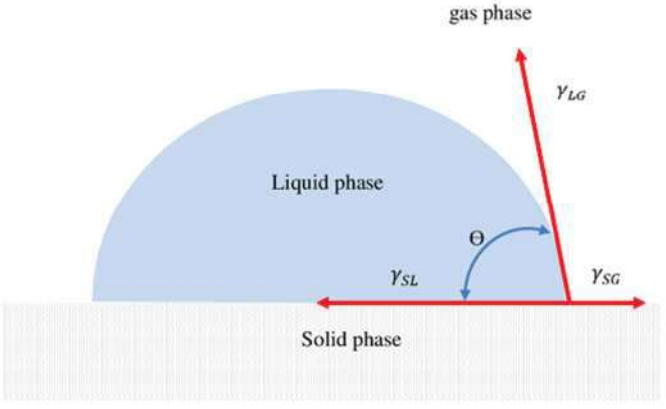

Fig. 1. Young model of droplet droplets on a flat, smooth surface and homogeneous

b) The Wenzel model (Fig. 2a)

Surface roughness (r) contributes significantly to wetting behaviour on solid, rough and homogeneous surfaces.

$$Cos\ \theta_r = r\ Cos\ \theta \quad (2)$$

The roughness factor (r) is a dimensionless parameter which is always greater than 1. Based on the Wenzel equation, if $\theta<\pi/2$ then $\theta r<\theta$ and if $\theta>\pi/2$ then $\theta r<\theta$. Therefore, in the Wenzel model, roughness can increase surface hydrophilicity that is initially wetted. Whereas on surfaces that are not initially wetted, roughness can make surfaces increasingly less wet, which causes an increase in their hydrophobicity [24]. Usually, water droplets tend to stick to surfaces that follow the wetting of the Wenzel model and will roll easily on surfaces that follow the Cassie and Baxter models [13,25-27].

c) Cassie-Baxter model (model for heterogeneous surfaces, Fig. 2b)

If f is the fractional area of the liquid in contact with solids, (*1 - f*) is the fractional area of air, with $\theta = 180°$ for air.

$$Cos\theta_c = f_1 cos\theta_1 + f_2 cos\theta_2 \quad (3)$$

The contact angle on a heterogeneous (porous) surface decreases with an increase in the wetted surface area (*f*).

$$Cos\theta_c = f\cos\theta + f - 1 \quad (4)$$

The phenomenon of gas trapped on the surface of taro leaves (Colocasia esculenta) has been investigated [28]. This research succeeded in uncovering the existence of hydrogen gas bubbles formed in the superhydrophobic process, this hydrogen gas is trapped in the nano surface gap of the leaf. The mechanism of the occurrence of hydrogen gas is the reaction between the elements contained in the leaf surface with droplet H_2O which is assisted by the surface energy of the superhydrophobic process. Based on this research shows the occurrence of superhydrophobic properties can be described chemically and physically. The chemical mechanism explains how the gas bubbles are trapped while the physical process, explains the super-hydrophobic nature according to the Cassie-Baxter model.

2. Material and method

2.1. Material

The materials used are nano-Magnesium particles (red arrows) with grain size: (800 nm), made in US Research Nano-materials, Inc. (the USA). Alumina nanoparticles (white arrows), size: (52.45 nm), brand: Merck, made in Germany. To reduce the amount of gas formed the percentage of Mg is varied by adding nano-Alumina particles in the following ratios (in %): (0:100, 10:90, 20:80, 30:70, 40:60, 50:50, 60:40, 70:30, 80:20, 90:10 and 100:0). The function of nano-Alumina particles is to provide a roughness effect on the surface and to vary the Mg content of the membrane.

Preparation of membrane manufacture by mixing the percentage of Mg and Al_2O_3 by with the comparison. Then the mixture of particles is put in a closed container and shaken until it is mixed homogeneously. After homogeneous sprinkling on the adhesive tape to form a membrane layer like Figure 3.

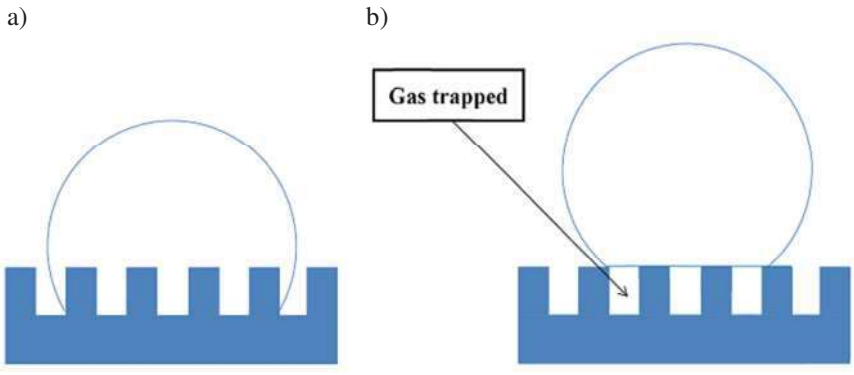

Fig. 2. a) Wenzel model (without trapped air), b) Cassie-Baxter model (with trapped air)

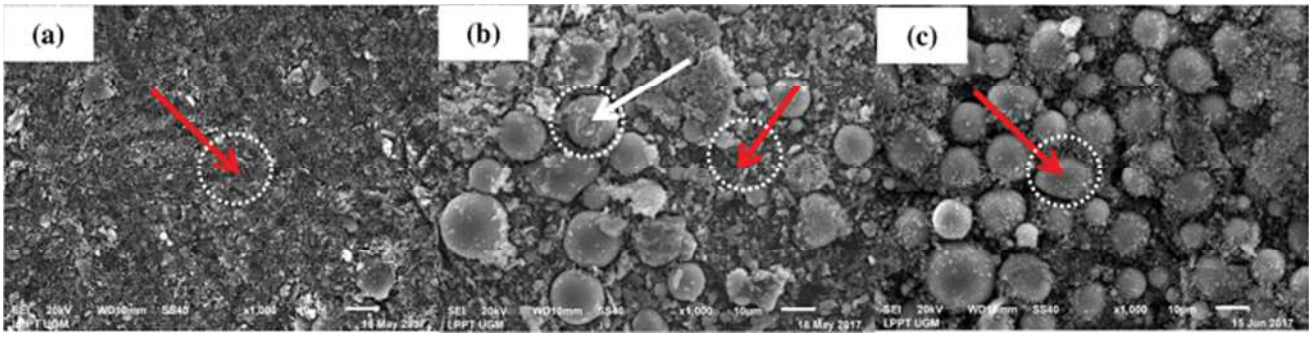

Fig. 3. Membrane samples in composition: (a) Mg membrane: 0%, (b) Mg membrane: 50% and (c) Mg membrane: 100%

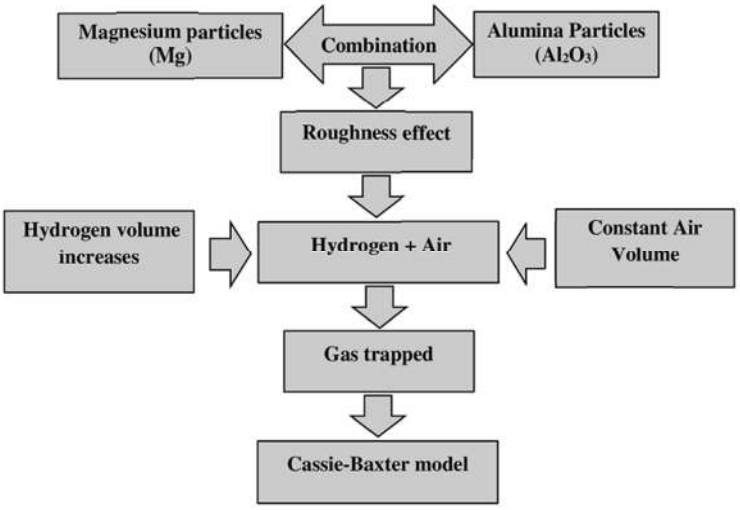

Fig. 4. Cassie-Baxter model on membranes Magnesium (Mg) and Alumina (Al_2O_3)

Mixed Magnesium (Mg) and Alumina (Al_2O_3) membranes have surface roughness at the nanoscale that causes trapped gas (Fig. 4). Then the nano-Magnesium particles are able to react with droplet H_2O to produce Hydrogen. This has been proven by the gas chromatography test results shown in Figure 5. This hydrogen volume can be increased by increasing the Mg presentation (0-100%) so that the optimum Cassie-Baxter model is achieved. The process of the reaction between Mg (s) and H_2O follows the reaction equation as follows:

$$Mg_{(s)} + 2H_2O \rightarrow Mg(OH)_2 + H_2 \quad (5)$$

2.2. Research procedure

Detection of hydrogen gas

Figure 5, shows the sample gas reaction between water droplets (H_2O) with the membrane surface examined by gas chromatography apparently containing hydrogen gas that is 3.831% (3831 ppm). The results of the visualization of the reaction between H_2O and magnesium particles are shown in Figure 10 (e). The process of collecting hydrogen gas is carried out by reacting hydrogen gas with Aqua in a closed container then taking the reaction results are placed in a vacuum tube. Gas samples in a vacuum tube are then tested using gas chromatography.

Measurement of droplet volume and contact angle

Droplet volume measurements are performed as shown in Figure 6, using a tool (7), droplet volume is varied from 1 to 5 ml. The droplet contact angle measurements were made with a microscope position (2) as shown in Figure 6. The results of the image are displayed on a notebook (1), then with software measurement the droplet contact angle measurements (6).

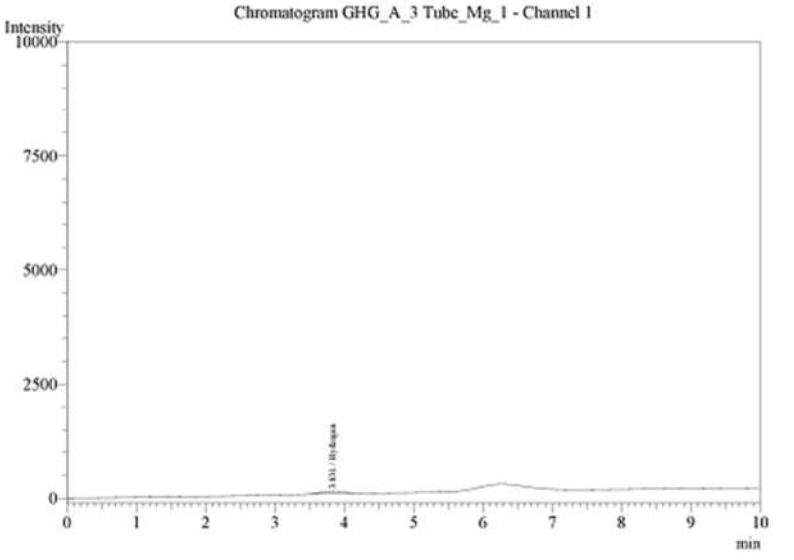

Peak Table - Channel 1

Peak#	Ret.Time	Area	Height	Conc.	Units	Mark	Name
1	3.831	1139	51	0.059	%		Hydrogen
Total		1139	51				

Fig. 5. Gas chromatography test results in the reaction between Magnesium particles and H_2O

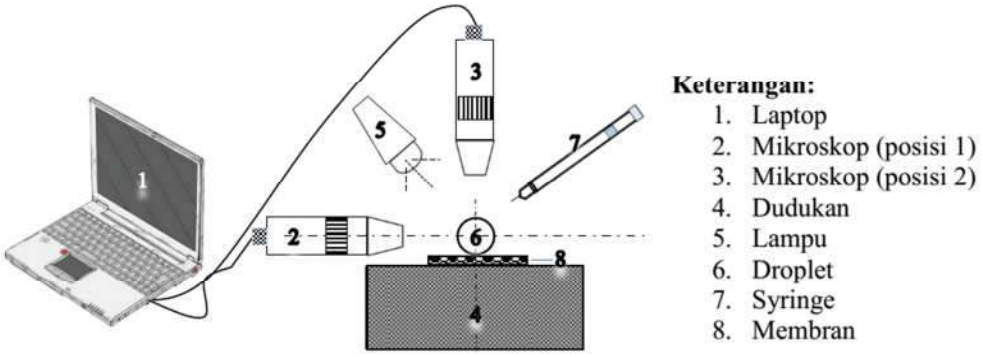

Fig. 6. Droplet measurement and image capture techniques with a digital microscope

Observation of hydrogen gas bubbles

Droplet volume measurements are performed as in Figure 6, using a device (7), the droplet volume varied (1-5 ml) dripped on the membrane (8). Taking pictures vertically on the droplet when contact is made with the position of the microscope (3) as in Figure 6. The results of the image are displayed on a notebook (1), then with the J-image software displayed on an mm scale.

Surface roughness measurement

Surface roughness analysis software: Gwyddion version: 2.54 released on August 27, 2019. The results of the measurement of roughness and 3-D analysis on the membrane surface are shown in Figures 8b), 9b) and 10b) and 8d), 9d) and 10d).

Calculation of Mg fractions on membranes (Al_2O_3 + Mg)

To adjust the number of Mg fractions of Figure 3b (red arrows) inside the Alumina layer Figure 3b (white arrows) is done by varying the amount of Mg/mm^2 in the Alumina area. Nano-Alumina and Magnesium particles are weighed according to their percentage: (0:100 mg, 10:90 mg, 20:80 mg, 30:70 mg, 40:60 mg, 50:50 mg, 60:40 mg, 70:30 mg, 80:20 mg, 90:10 mg and 100:0 mg).

3. Results and discussion

Figure 7, shows that there are three regions that are formed when the Magnesium percentage is varied (0-100%), namely: Hydrophobic region (blue ellipse sign), Superhidrophobic (black ellipse sign) and Hydrophilic (green ellipse sign). Figure 7, shows an interesting thing when the volume of trapped gas increases with increasing Mg fraction. Hydrophobic nature occurs when the layer at a concentration of 100% Alumina due to the trapped gas is constant is only caused by the effect of surface roughness. Magnesium condition of 50% is able to show superhydrophobic nature, this is due to the increased trapped gas volume and reaching the optimum point. At the percentage of Magnesium 100%, the opposite happens when the mixed membrane turns to hydrophilic due to the amount of gas volume that continues to increase so that the surface tension is getting weaker and the carrying capacity of the droplet above is getting weaker too.

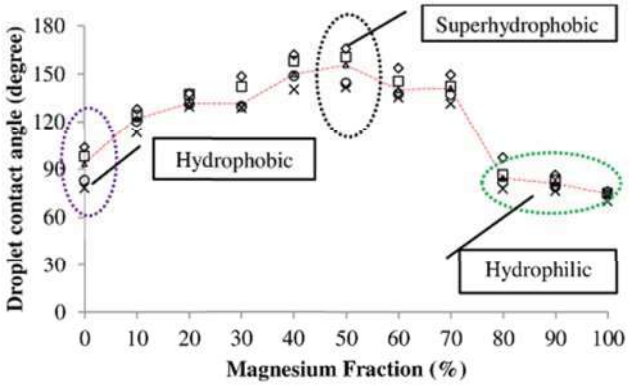

Fig. 7. Graph of the relationship between the Mg fraction and the droplet contact angle

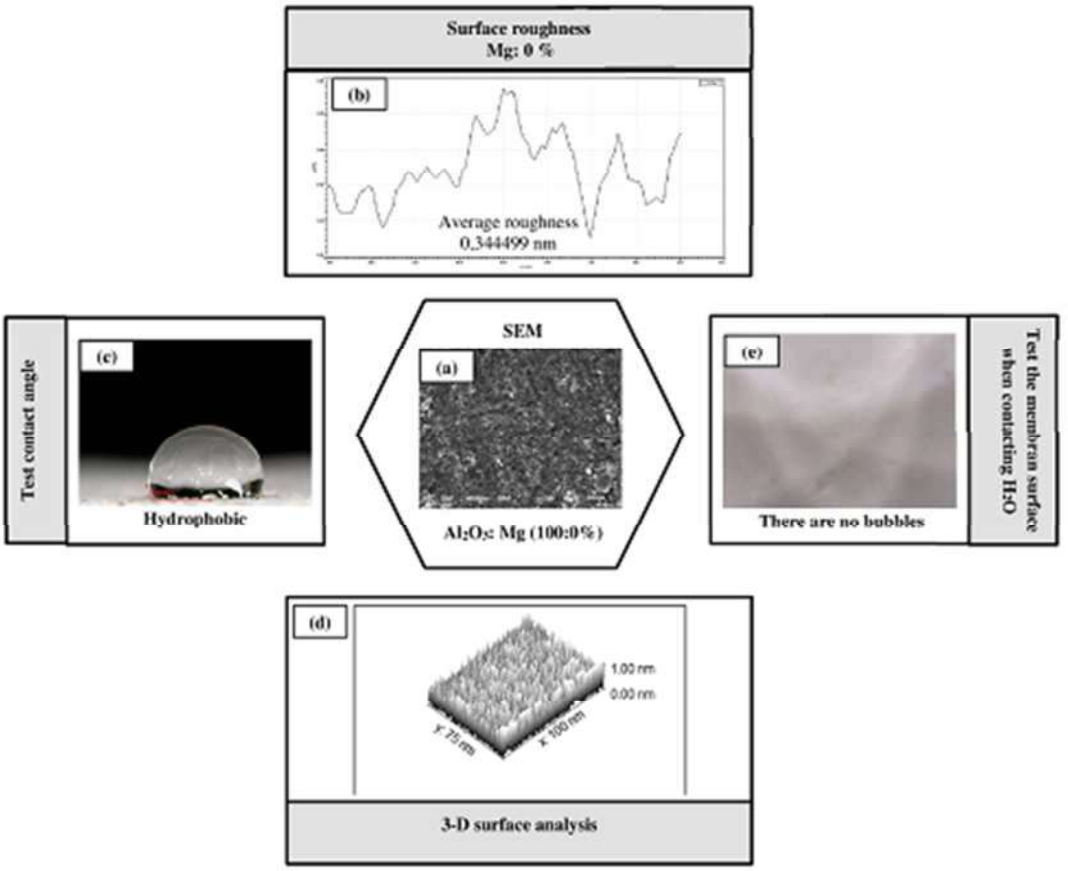

Fig. 8. Observation results on the hydrophobic membrane: a) Membrane surface SEM results, b,d) Measurement of roughness and 3-D, c) analysis contact angle contact with a droplet, e) Observation of bubbles with a digital microscope

The hydrophobic process is shown in Figure 8, the contact angle test results show the hydrophobic nature of Alumina (Al_2O_3) with 90° contact angles as shown in Figure 8c. Observations on the surface of the Alumina layer when droplet contact showed no appearance of bubbles as shown in Figure 8e. This shows that the gas trapped in the nano-gap in Figure 8b,d does not exceed its capacity so that bubbles do not appear when observed using a digital microscope. This is supported by the results of surface roughness measurements that show a low level of roughness so that the surface tension created is low, the constant buoyancy force of the trapped gas is weaker than the compressive force of the thin film droplet so that the gas sinks at the bottom of the grooves.

The superhydrophobic process occurs at an Alumina: Mg concentration (50:50%) SEM test results are shown in Figure 9a. The droplet contact angle test shows superhydrophobic nature where the contact angle of the droplet reaches 166°. The superhydrophobic nature of the mixed membrane is supported by surface roughness as shown in Figure 9b. The surface observations show a high level of roughness with sharp peaks of nanoparticles followed by valleys stretching along the mixed membrane. Gas is trapped in valleys that fill the entire space optimally, nano peaks are very sharp to support the droplet that is above it, creating very high surface tension. This is what influences the superhydrophobic nature of the mixed membrane. The difference with Alumina membranes is the presence of additional Hydrogen gas which is formed and accumulated in nano valleys which amplifies the pressure. The optimal pressure occurs in the composition of Mg: 50% which can increase the hydrophobic nature to become superhydrophobic.

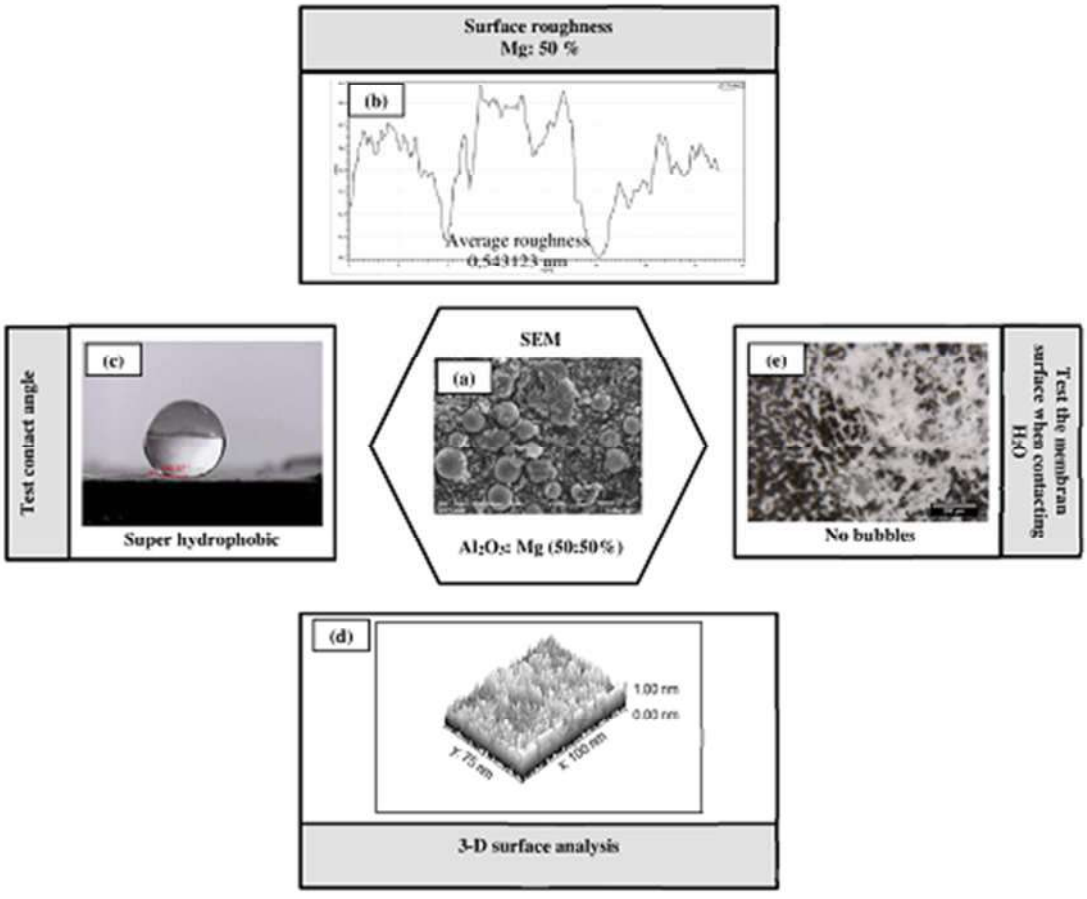

Fig. 9. Observation results in superhydrophobic membranes: a) Membrane surface SEM results, b,d) Measurement of roughness and 3-D, c) analysis Contact Angle contact with a droplet, e) Observation of bubbles with a digital microscope

Increasing the amount of Mg (50-100%) gives the effect of decreasing the contact angle as shown in Figure 10c this is caused by the Hydrogen gas bubbles that appear like Figure 10e when the droplet is in contact with the membrane. The appearance of bubbles on the surface of the Mg membrane: 100% is caused by the capacity of the hydrogen gas which continues to increase along with the reaction of Mg with H_2O so that the space of grooves space of Figure 10b is fully filled pressing the surface of the thin membrane droplet so that bubbles form outside the grooves as shown in Figure 10e. When the membrane surface is filled with bubbles the peaks of nanoparticles (circular marks) in Figure 10b are closed causing the effect of concentrated surface tension on the peaks of nanoparticles to weaken so that the contact angle of the droplet decreases as shown in Figure 10c.

3.1. Physical models based on gas pressure trapped on the membrane surface

When H_2O droplets come in contact with Magnesium, Alumina and mixed membranes (Magnesium + Alumina) which have roughness on their surface, the gas is trapped. This is caused by the surface tension of the liquid (γ) which resembles a thin membrane covering the grooves on its surface. The stress on the droplet when in contact with the surface is formulated as follows (Fig. 11):

$$\gamma = \frac{\text{Downward pressure}(F\downarrow)}{\text{Droplet diameter}(d)} \tag{6}$$

Equation (6), can also be written as follows:

$$F\downarrow = \gamma . d \tag{7}$$

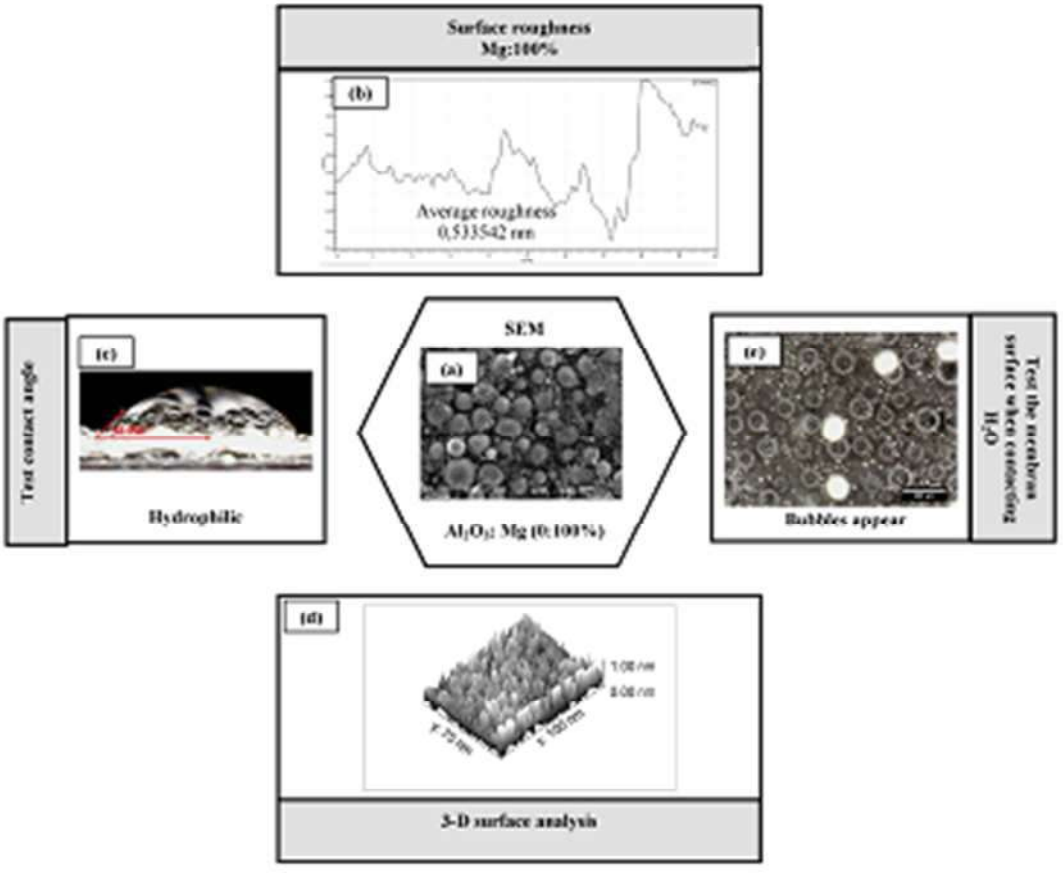

Fig. 10. Observation results on Hydrophilic membrane: (a). Membrane surface SEM results (b, d). Measurement of roughness and 3-D (c). Analysis Contact Angle contact with a droplet (e). Observation of bubbles with a digital microscope

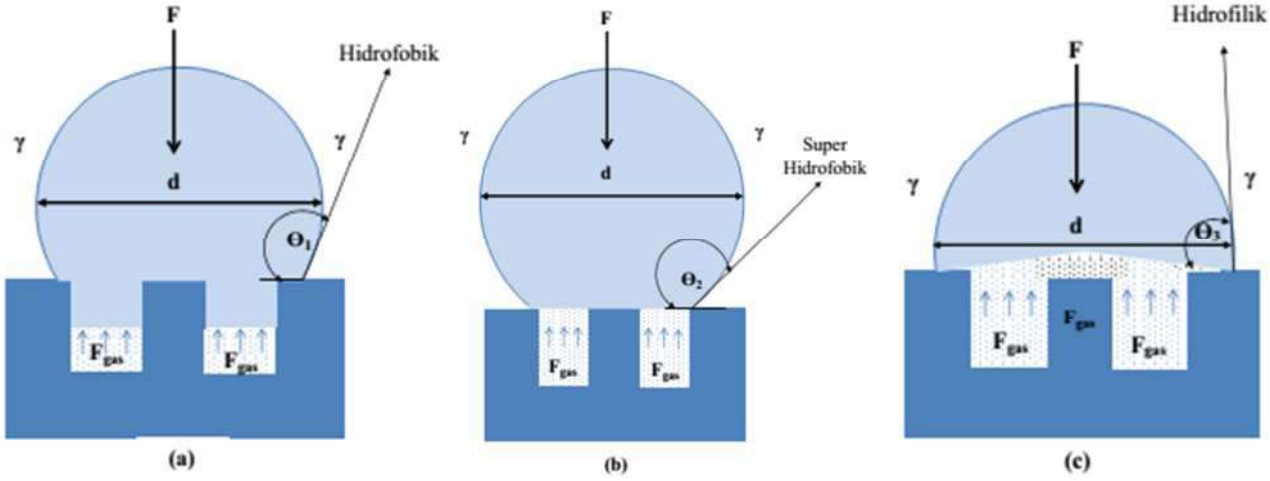

Fig. 11. a) Hydrophobic conditions, b) Superhydrophobic condition, c) Hydrophilic condition

Gases trapped in surface roughness like Figure 11, have an upward buoyancy force (Buoyancy) following the equation as follows:

$$F_{gas} \uparrow = P_{gas} \,.A \tag{8}$$

where,
Gas = gas pressure, N / m^2,
A = droplet cross-sectional area, m^2.

The equilibrium of forces from equations (7) and (8) are:

$$\sum F_{(\text{resultan force})} = 0$$

$$F_{gas} \uparrow - F \downarrow = 0$$

$$F_{gas} \uparrow = F \downarrow$$

Gas trapped force = droplet compressive force.

From the equation above shows there are three conditions that occur when droplets come in contact with membranes, namely:

a) Hydrophobic conditions when the trapped gas pressure is smaller than the droplet pressure (F-gas ↑ <F ↓), this causes the trapped gas has not been maximized in supporting the hydrophobicity of the membrane as shown in Figure 11a.
b) The superhydrophobic condition when gas pressure is trapped equally to droplet pressure (F-gas ↑ = F ↓). In this condition, there is a force balance between the droplet compressive force and the upward gas force, this causes the grooves to be filled with gas and the droplet is directly above the pointed peaks of the membrane particles as shown in Figure 11b.
c) Hydrophilic conditions occur when the pressure of the trapped gas is greater than the downward pressure droplet (Fgas> F ↓). This causes the gas bubbles to exceed the capacity of the grooves and cover the sharp peaks of the membrane particles so that the surface tension of the droplet decreases and turns into hydrophilic as shown in Figure 11c.

3.2. The physical model is based on the Cassie-Baxter equation

The emergence of Hydrogen and Air-gas trapped in grooves as shown in Figure 12. This trapped gas follows the Cassie-Baxter interface which plays a role in superhydrophobic properties. Surface roughness is a non-dimensional factor (R_f) and the surface area ratio is the ratio between (solid-liquid surface area/flat surface area), so the contact angle values are formulated as follows:

$$\cos\theta = \frac{dA_{LA}}{dA_F} = \frac{A_{SL}}{A_F}\frac{dA_{LA}}{dA_{SL}} = R_F \cos\theta_0 \tag{9}$$

Surface roughness (R_f) on a micro/nano-meter scale reinforces the hydrophobicity of the membrane. A hydrophobic membrane surface will become more hydrophobic when it's surface roughness increases. Whereas the surface of the hydrophilic membrane becomes more hydrophilic if the surface roughness increases [24-26].

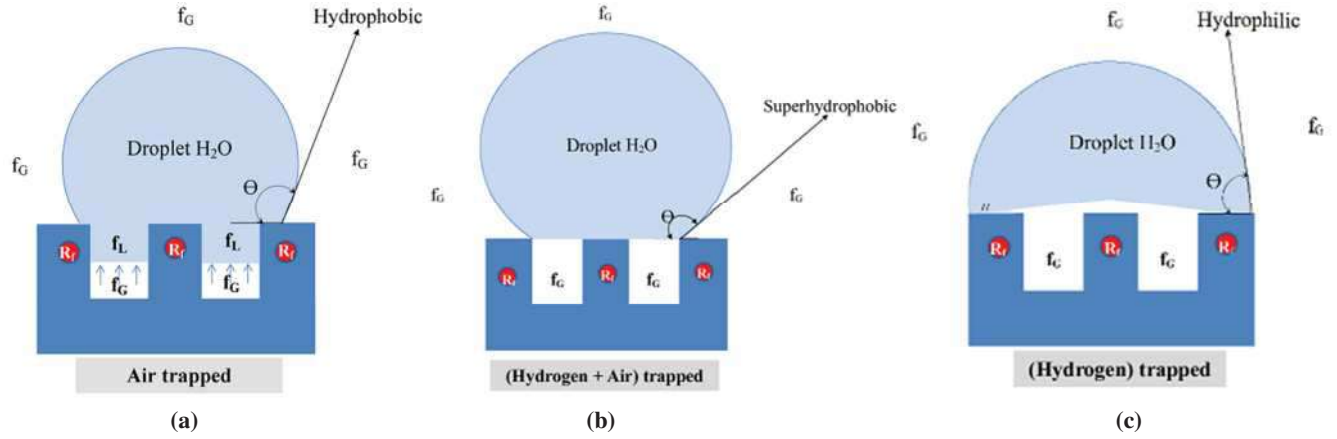

Fig. 12. Physical mechanism model based on the Cassie-Baxter equation: a) Hydrophobic, b) Superhydrophobic and c) Hydrophilic

For surfaces consisting of two fractions like Figure 12, the first fraction with the solid-liquid fraction area (f_1) with contact angle θ_1 and the second fraction with the liquid-gas fraction area (f_2) with contact angle θ_2 the contact angle equation is :

$$\text{Cos}\ \theta = f_1 \cos\theta_1 + f_2 \cos\theta_2 \tag{10}$$

In the case of a membrane interface consisting of a solid-liquid fraction ($f_1 = f_{SL}$, $\Theta_1 = \Theta_2$) and a liquid-gas fraction ($f_1 = f_{LG} = 1 - f_{SL}$, Cos $\Theta_2 = -1$), by combining equation (9) and (10) produces the equation:

$$\text{Cos}\ \theta = R_f\, f_{SL} \cos\theta_0 - 1 + f_{SL} \tag{11}$$

To determine the effect of the liquid-gas fraction, substitution ($f_{SL} = 1 - f_{LG}$) so that it becomes:

$$\begin{aligned}\text{Cos}\ \theta &= R_f\,(1 - f_{LG})\cos\theta_0 - 1 + 1 - f_{LG} \\ &= (R_f - R_f\,.\,f_{LG})\cos\theta_0 - 1 + 1 - f_{LG} \\ &= R_f \cos\theta_0 - R_f\,.\,f_{LG}.\cos\theta_0 - 1 + 1 - f_{LG} \\ \text{Cos}\ \theta &= R_f \cos\theta_0 - f_{LG}(R_f \cos\theta_0 + 1)\end{aligned} \tag{12}$$

The results of physical mechanism models show that the hydrophobicity of a membrane is very dependent on: the value of surface roughness (R_f), the liquid-gas fraction (f_{LG}) and the ratio between liquid-gas/solid-liquid contact (cos θ_0). Specifically, in the liquid-gas fraction (f_{LG}) there are three models when we add to the pressure of trapped gas namely:

a. Gas model (Air), when H_2O droplet comes in contact with Alumina membrane due to surface roughness, it causes gas to get trapped. The hydrophobicity of this membrane does not increase because the amount of the trapped gas fraction remains unchanged as shown in Figure 12a.
b. Gas model (Air + Hydrogen), when droplet H_2O comes in contact with the membrane (Mg + Alumina) the reaction produces Hydrogen gas whose volume continues to increase as shown in Figure 12b. The hydrogen gas fraction continues to increase until lifting the droplet upward reaches superhydrophobic properties.
c. Gas model (Hydrogen) when H_2O droplet comes in contact with the membrane, the reaction results in excessive hydrogen gas fraction resulting in the gas impulse being trapped so strongly that the bubbles grow outside the grooves and damage its hydrophobicity as shown in Figure 12c.

4. Conclusions

a) Hydrophobic properties occur when membranes at Alumina concentrations: 100% this is caused by gases trapped under constant conditions. The condition of Magnesium 50% is able to show superhydrophobic nature, this is caused by the volume of trapped gas which increases and reaches its optimum point. At the percentage of Magnesium 100%, the opposite occurs when the membrane turns to hydrophilic due to the amount of gas volume that continues to increase so that

the surface tension is weakening and the carrying capacity of the droplets above is also weakening.

b) There are three conditions that occur when droplets come in contact with the membrane layer, namely:
   - Hydrophobic conditions when the trapped gas pressure is smaller than the droplet pressure (F-gas ↑ <F ↓), this causes the trapped gas has not been maximized in supporting the hydrophobicity of the membrane.
   - Superhydrophobic conditions when trapped gas pressure equals droplet pressure (F-gas ↑ = F ↓). In this condition there is a force balance between the droplet compressive force and the upward gas force, this causes the grooves to be filled with gas and the droplet is directly above the pointed peaks of the membrane particles.
   - Hydrophilic conditions occur when the pressure of the trapped gas is greater than the downward pressure droplet (F-gas> F ↓). This causes the gas bubbles to exceed the capacity of the grooves and cover the sharp peaks of the membrane particles so that the surface tension of the droplet decreases and turns into hydrophilic.

c) A physical model based on the Cassie-Baxter equation:
   - Gas (Air) model, when H_2O droplet contact with the membrane results in air being trapped. The hydrophobicity of this membrane does not increase because the amount of air fraction is trapped constantly.
   - Gas model (Air + Hydrogen), when droplet H_2O comes in contact with the membrane (Mg + Alumina) the reaction produces Hydrogen gas whose volume continues to increase. The hydrogen gas fraction continues to increase until lifting the droplet upward reaches superhydrophobic properties.
   - Gas (Hydrogen) model when H_2O droplet comes in contact with the membrane, the reaction results in excessive hydrogen gas fraction resulting in the gas impulse being trapped so strongly that the bubbles grow outside the grooves and damage its hydrophobicity.

References

[1] A.V. Adamson, Physical Chemistry of Surfaces, Wiley, New York, 1990, DOI: https://doi.org/10.1080/01932699108913152.

[2] J.N. Israelachvili, Intermolecular and Surface Forces, Second Edition, Academic Press, London, 1992, DOI: https://doi.org/10.1080/01932699208943350.

[3] B. Bhushan, Principles and Applications of Tribology, Wiley, New York. 1999, DOI: http://dx.doi.org/10.1007/978-*3*-540-78425-8.

[4] B. Bhushan, Introduction to Tribology, Wiley, New York, 2002, DOI: https://doi.org/10.1115/1.1523360.

[5] B. Bhushan, Nanotribology and Nanomechanics – An Introduction, Second Edition, Springer-Verlag, Heidelberg, Germany, 2008, DOI: https://doi.org/10.1007/978-3-540-77608-60.

[6] M. Nosonovsky, B. Bhushan, Multiscale Dissipative Mechanisms and Hierarchical Surface: Friction, Superhydrophobicity, and Biomimetics, Springer-Verlag, Heidelberg, Germany, 2008, DOI: https://doi.org/10.1007/978-3-540-78425-8.

[7] T. Onda, S. Shibuichi, N. Satoh, K. Tsujii, Super-Water-Repellent Fractal Surfaces, Langmuir 12 (1996) 2125-2127, DOI: https://doi.org/10.1021/la950418o.

[8] A. Nakajima, K. Hashimoto, T. Watanabe, K. Takai, G. Yamauchi, A. Fujishima, Transparent superhydrophobic thin films with self-cleaning properties, Langmuir 16/17 (2000) 7044-7047, DOI: https://doi.org/10.1021/la000155k.

[9] C. Cottin-Bizonne, J.L. Barrat, L. Bocquet, E. Charlaix, Low-friction flows of liquid at nanopatterned interfaces, Nature Materials 2/4 (2003) 237-240, DOI: https://doi.org/10.1038/nmat857.

[10] R. Truesdell, A. Mammoli, P. Vorobieff, F. van Swol, C.J. Brinker, Drag Reduction on a Patterned Superhydrophobic Surface, Physical Review Letters 97/4 (2006)c44504, DOI: https://doi.org/10.1038/s41598-017-16369-3.

[11] B. Bhushan, Biomimetics: Lessons from Nature – An Overview, Philosophical Transactions of the Royal Society A 367 (2009) 1445-1486, DOI: https://doi.org/10.1098/rsta.2009.0011.

[12] K. Koch, B. Bhushan, W. Barthlott, Multifunctional Surface Structures of Plants: An Inspiration for Biomimetics, Progress in Materials Science 54/2 (2009) 137-178, DOI: https://doi.org/10.1016/j.pmatsci.2008.07.003.

[13] P. Roach, N.J. Shirtcliffe, M.I. Newton, Progess in superhydrophobic surface development, Soft Matter 4 (2008) 224-240, DOI: https://doi.org/10.1039/B712575P.

[14] E. Khalili, M. Sarafbidabad, Combination of laser patterning and nano PTFE sputtering for the creation a super-hydrophobic surface on 304 stainless steel in medical applications, Surfaces and Interfaces 8 (2017) 219-224, DOI: https://doi.org/10.1016/j.surfin.2017.06.008.

[15] K. Jeyasubramanian, G.S. Hikku, A.V.M. Preethi, V.S. Benitha, N. Selvakumar, Fabrication of water repellent

cotton fabric by coating nano particle impregnated hydrophobic additives and its characterization, Journal of Industrial and Engineering Chemistry 37 (2016) 180-189, DOI: https://doi.org/10.1016/j.jiec.2016.03.023.

[16] H. Yan, X. Lu, C. Wu, X. Sun, W. Tang, Fabrication of a super-hydrophobic polyvinylidene fluoride hollow fiber membrane using a particle coating process, Journal of Membrane Science 533 (2017) 130-140, DOI: https://doi.org/10.1016/j.memsci.2017.03.033.

[17] Y. He, W.T. Sun, S.C. Wang, P.A.S. Reed, F.C. Walsh, An electrodeposited Ni-P-WS_2 coating with combined super-hydrophobicity and self-lubricating properties, Electrochimica Acta 245 (2017) 872-882, DOI: https://doi.org/10.1016/j.electacta.2017.05.166.

[18] Sh. Ammar, K. Ramesh, B. Vengadaesvaran, S. Ramesh, A.K. Arof, A novel coating material that uses nano-sized SiO_2 particles to intensify hydrophobicity and corrosion protection properties, Electrochimica Acta 220 (2016) 417-426, DOI: https://doi.org/10.1016/j.electacta.2016.10.099.

[19] E. Celia, T. Darmanin, E. Taffin de Givenchy, S. Amigoni, F. Guittard, Recent advances in designing superhydrophobic surfaces, Journal of Colloid and Interface Science 402 (2013) 1-18, DOI: https://doi.org/10.1016/j.jcis.2013.03.041.

[20] J. Drelich, E. Chibowski, D.D. Meng, K. Terpilowski, Hydrophilic and superhydrophilic surfaces and materials, Soft Matter 7 (2011) 9804-9828, DOI: https://doi.org/10.1039/C1SM05849E.

[21] R.J. Good, Contact angle, wetting, and adhesion: a critical review, Journal of Adhesion Science and Technology 6/12 (1992) 1269-1302, DOI: https://doi.org/10.1163/156856192X00629.

[22] Z. Xu, X. Huang, L. Wan, Surface Engineering of Polymer Membranes, Springer Berlin Heidelberg, New York, 2009.

[23] B. Wang, Y. Zhang, L. Shi, J. Li, Z. Guo, Advances in the theory of superhydrophobic surfaces, Journal of Materials Chemistry 22 (2012) 20112-20127, DOI: https://doi.org/10.1039/C2JM32780E.

[24] M. Nosonovsky, B. Bhushan, Roughness optimization for biomimetic superhydrophobic surfaces, Microsystems Technology 11/7 (2005) 535-549, DOI: https://doi.org/10.1007/s00542-005-0602-9.

[25] Y.C. Jung, B. Bhushan, Contact Angle, Adhesion, and Friction Properties of Micro- and Nanopatterned Polymers for Superhydrophobicity, Nanotechnology 17/19 (2006) 4970-4980, DOI: https://doi.org/10.1088/0957-4484/17/19/033.

[26] R.N. Wenzel, Resistance of Solid Surface to Wetting by Water, Industrial & Engineering Chemistry 28 (1936) 988-994, DOI: https://doi.org/10.1021/ie50320a024.

[27] A.B.D. Cassie, S. Baxter, Wettability of porous surfaces, Transactions of the Faraday Society 40 (1944) 546-551, DOI: https://doi.org/10.1039/TF9444000546.

[28] R. Subagyo, I.N.G. Wardana, A. Widodo, E. Siswanto, The mechanism of hydrogen bubble formation caused by the superhydrophobic characteristic of taro leaves, International Review of Mechanical Engineering (IREME) 11/2 (2017) 95-100, DOI: https://doi.org/10.15866/ireme.v11i2.10621.